

Inferring Structural Ensembles from Noisy Experiments

Kyle A. Beauchamp,[†] Rhiju Das^{†,‡} and Vijay S. Pande^{†*,¶}

Biophysics Program, Biochemistry Department, Stanford University, Stanford, CA, and Chemistry Department, Stanford University, Stanford, CA

E-mail: rhiju@stanford.edu, pande@stanford.edu

Abstract

Inferring conformation from experiment is the fundamental task of structural biology. Due to limited experimental resolution, structure determination often requires a combination of modelling and experiment. Current algorithms for structure determination, however, are limited to modelling a single conformation and provide only limited uncertainty information. Here we describe linear virtual biasing potential (LVBP), a method that combines simulation and experiment to infer solution ensembles. By using the machinery of Bayesian statistics, LVBP gives rigorous uncertainty estimates for structural features and equilibrium properties. Using trialanine as a test system, we show that LVBP corrects forcefield error and outperforms previous analysis methods.

*To whom correspondence should be addressed

[†]Biophysics Program

[‡]Biochemistry Department

[¶]Chemistry Department

Introduction

Over the past forty years, structural biologists have solved “ground-state” structures of countless biological macromolecules.¹ Modern biology, however, presents many systems that do not fit the single-structure paradigm—excited states of nucleic acids,² natively disordered proteins,³ and protein folding intermediates⁴ alike are poorly described by single conformation models. For such systems, conformational ensembles provide a rigorous framework for understanding structural and equilibrium properties.

Here we introduce a statistical approach to modelling solution ensembles of biological macromolecules. The algorithm, Linear Virtual Biasing Potential (LVBP), uses solution experiments to reweight a collection of atomistic models. In LVBP, Bayesian inference transforms experimental ambiguity into error bars on arbitrary structural features.

To validate LVBP, we investigate two model systems. We first use NMR data to infer conformational ensembles of trialanine.⁵ We construct ensembles using five molecular dynamics forcefields with differing conformational propensities. LVBP corrects forcefield errors to provide self-consistent estimates of the α , β , and PP_{II} populations.

Theory: Linear Virtual Biasing Potential

Model Inputs

To model an ensemble using LVBP requires three components (Fig. 1). First, we need a set of conformations (x_j) sampled from the approximate equilibrium distribution of our system. In the present work, such conformations will be generated from molecular dynamics (MD) simulations. Second, we require a set of equilibrium experimental measurements (F_i) and their associated uncertainties (σ_i). Third, it is necessary to have a direct connection between simulation and experiment. This connection is achieved by predicting each experimental observable at each conformation: $f_i(x_j)$ is the predicted value of experiment i at conformation x_j .

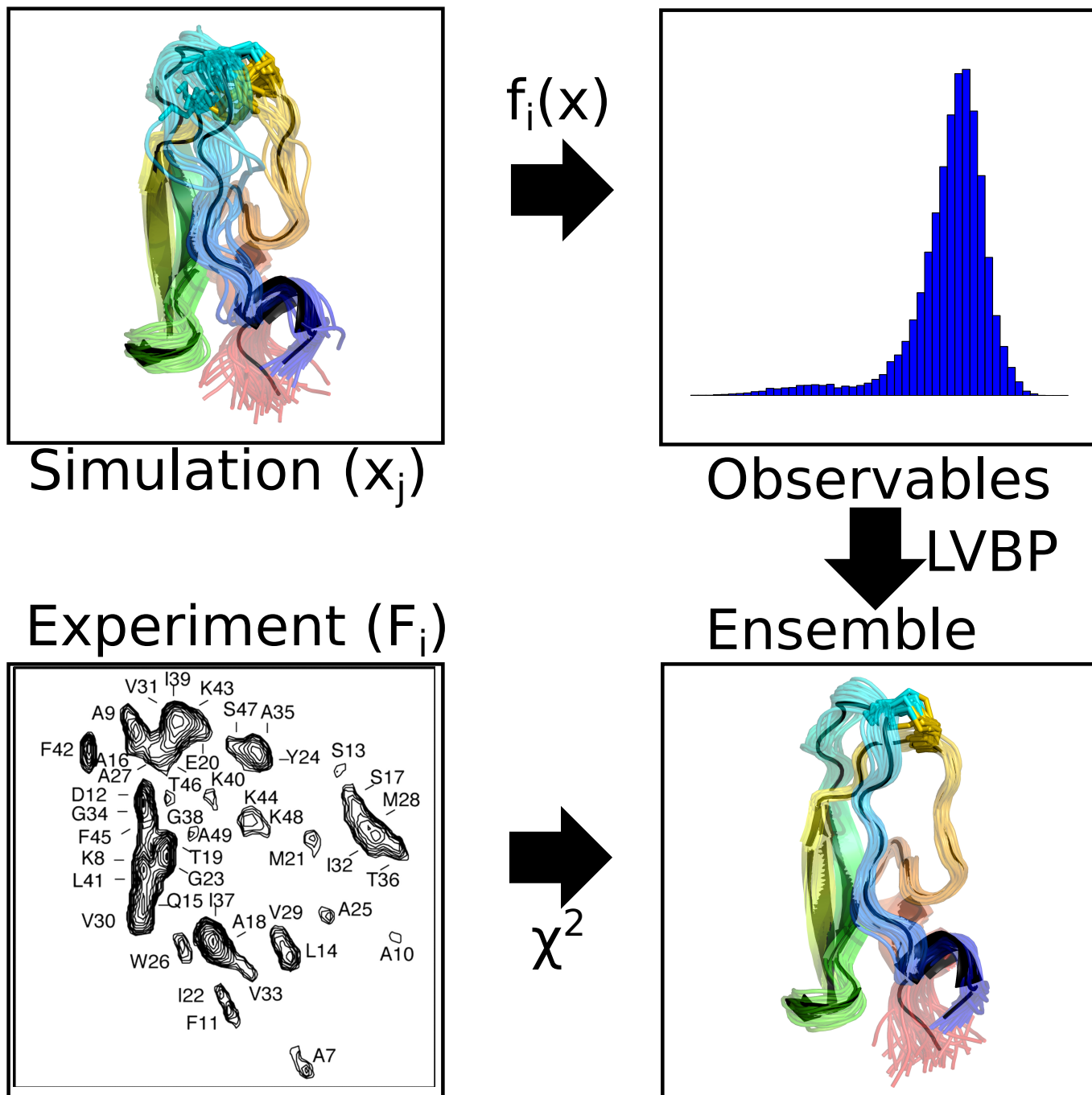


Figure 1: General scheme for LVBP modelling.

Reweightings

The next step in constructing an ensemble is to calculate the population of each conformation. For convenience, we work with the log populations (i.e. free energies). Inspired by a previous method for restraining simulations,⁶ we reweight individual conformations by a biasing potential that is a linear combination of the predicted observables:

$$\Delta U(x; \alpha) = \sum_i^n \alpha_i f_i(x)$$

In $\Delta U(x; \alpha)$, the parameters α_i determine how strongly each experiment contributes to the biasing potential. One way to think about α is via “tilting” the energy landscape along the order parameters $f_i(x)$. Given the biasing potential, the population of each conformation can be calculated using exponential averaging (see Appx. S1):

$$\pi_j(\alpha) = \frac{1}{\sum_k \exp[-\Delta U(x_k; \alpha)]} \exp[-\Delta U(x_j; \alpha)]$$

It is informative to consider the case of a single observable $f(x)$. Suppose the molecule of interest shows a normally distributed observable. If we let $\alpha = 0$, then the biasing potential is 0 everywhere and our reweighted ensemble simply returns the results of the MD simulation (Fig. 2b). However, if we let $\alpha = -2$, conformations with large values of $f(x)$ are upweighted, while conformations with lower values of $f(x)$ are downweighted (Fig. 2a). Finally, if $\alpha = +2$, the ensemble shifts in the opposite direction (Fig. 2c).

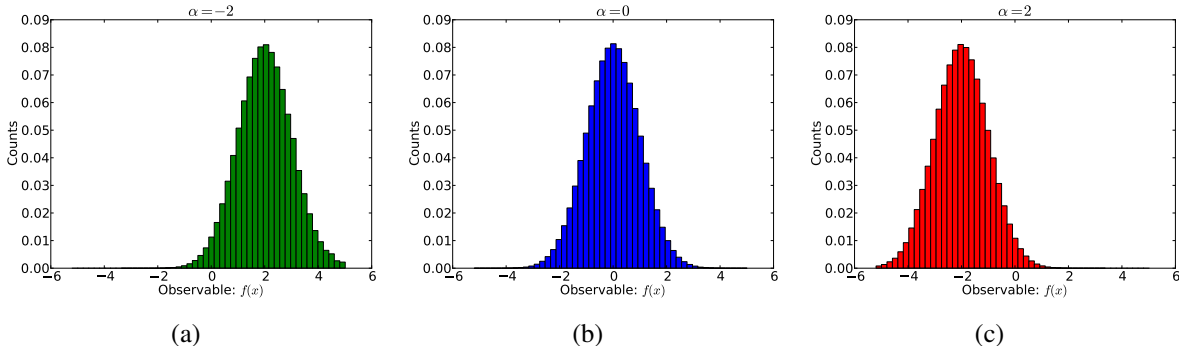


Figure 2: Raw ($\alpha = 0$) and reweighted histograms of a one dimensional observable.

With the equilibrium populations, we can calculate the equilibrium expectations of an arbitrary observable $h(x)$:

$$\langle h(x) \rangle_{\alpha} = \sum_j h(x_j) \pi_j(\alpha)$$

In the above bracket notation, $\langle h(x) \rangle_{\alpha}$ is the ensemble average of $h(x)$ in an ensemble that is perturbed by a biasing potential $\Delta U(x; \alpha)$. At this point, the determination of α has not yet been discussed. The key idea, however, is that the α reweighted ensemble $\langle \rangle_{\alpha}$ should recapitulate the experimental measurements:

$$\langle f_i(x) \rangle_{\alpha} \approx F_i$$

A likelihood framework

We now derive a likelihood framework for determining the coefficients α used in the biasing potential. Given adequate sampling and self-consistent experiments, there should exist some *true* value of α whose ensemble matches the experimental data. However, experimental uncertainty (σ_i) prevents exact agreement between the measurements and the true ensemble. For the models in the current work, we model σ_i as the uncertainty associated with predicting chemical shifts and scalar couplings from structures; this dominant error is quantified by the RMS uncertainty estimated during the parameterization of chemical shift and scalar coupling models. We use an independent normal approximation (see Appx. S2) to model the agreement between the α ensemble and the measurements:

$$P(F_i | \alpha) \sim N(\langle f_i(x) \rangle_{\alpha}, \sigma_i^2)$$

Using Bayes Theorem, we can calculate the likelihood of α given the measurements:

$$P(\alpha | F_1, \dots, F_n) \propto P(F_1, \dots, F_n | \alpha) P(\alpha)$$

Now we let $LL(\alpha)$ denote the log likelihood of α and simplify, dropping terms that are independent of α :

$$LL(\alpha) = \log[P(\alpha|F_1, \dots, F_n)] = -\sum_i \frac{1}{2\sigma_i^2} (\langle f_i \rangle_\alpha - F_i)^2 + \log P(\alpha)$$

Note the simple form of the log likelihood. The first term measures the χ^2 agreement between the reweighted ensemble and measurements. The second term is the log of the prior distribution on α . Although other priors are possible (see Appxs. S3, S4), we recommend a maximum entropy prior, which penalizes ensembles as they deviate from the raw simulation results:

$$\log P(\alpha) = \lambda \sum_j \pi_j(\alpha) \log \pi_j(\alpha)$$

With large values of λ , the maximum entropy prior favors the raw simulation results (i.e. uniform conformational populations): $\pi_i \approx \frac{1}{n}$. The value of λ can be chosen via cross-validation or other methods (see Appx. S5).

Bayesian Modeling of Structural Ensembles

Because ensemble inference often presents many plausible solutions,^{7,8} we avoid statistical methods that return a single solution (e.g. maximum likelihood). We therefore use Markov chain Monte Carlo (MCMC), as implemented in PyMC,⁹ to sample the distribution of structural ensembles consistent with experiment. The result is an ensemble of ensembles—a statistical ensemble of conformational ensembles. Averaging all MCMC samples provides posterior mean estimates of arbitrary structural features. Similarly, examining the MCMC variances provides statistical uncertainties. The shape of the posterior distribution indicates whether one or several models are consistent with the available data (Fig. S1). A Bayesian bootstrapping procedure¹⁰ can also be used to model the statistical uncertainty of the MD simulations (see Appx. S6).

Results

Conformational Propensities of Trialanine

Short peptides provide crucial tests for evaluating and optimizing molecular dynamics force-fields.^{5,11–14} Such peptides offer a window into the intrinsic conformational propensities of amino acids, free from the secondary structure bias found in statistical surveys of protein structures.¹⁵ Here, we use LVBP to infer the conformational populations of trialanine from chemical shift and scalar coupling measurements.⁵

Trialanine was simulated (see Methods) in five different force fields; nine experimental measurements (six scalar couplings, three chemical shifts) probing the central ALA residue were used to construct an LVBP ensemble. The five force fields show considerable variation in their agreement with experiment (Fig. 3a). The amber96, amber99, charmm27, and oplsa forcefields, for example, initially show significant deviation from the experimental measurements. Upon reweighting, however, all five forcefields agree with experiment.

Previous experimental studies have shown that short alanine peptides prefer the polyproline type helix (PPII) in solution.^{5,14,16} Most molecular dynamics forcefields, however, are known to underpopulate the PPII state.^{5,11–13} Our trialanine simulations recapitulate this known deficiency (Fig. 3 b-d; blue), with amber96 showing a strong β bias and amber99 showing a strong α bias. However, combining simulation and experiment leads to conformational ensembles that are robust to forcefield differences (Fig. 3 b-d, green; Fig. S2). Reweighting with limited experimental data is a powerful technique for correcting forcefield deficiencies.

Discussion

Structural (Ensemble?) Biology

Why model structural ensembles, rather than just structures? At least three compelling reasons favor ensembles. First, biological molecules are multi-state machines; they fold, unfold, bind lig-

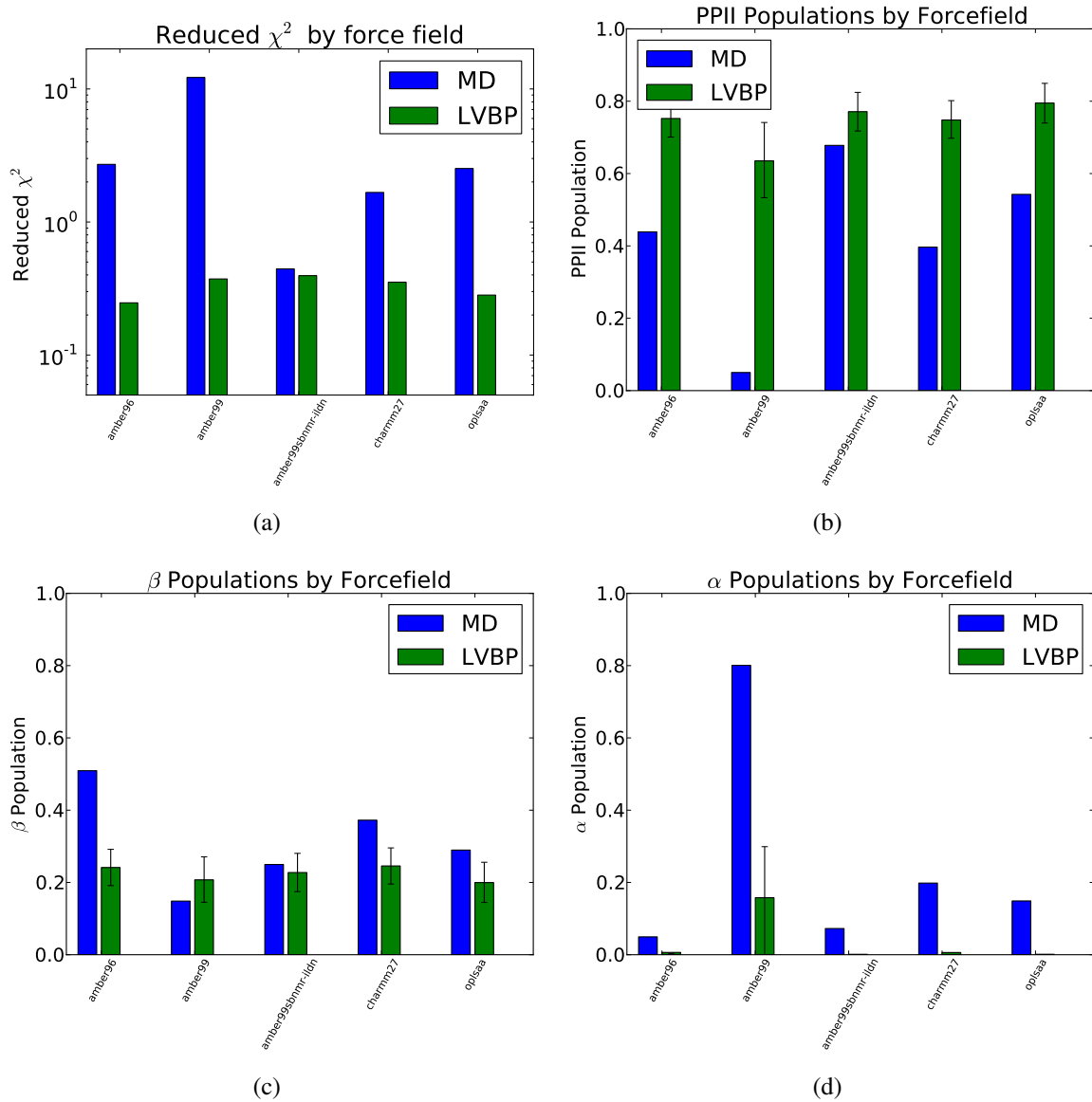


Figure 3: (a). The reduced χ^2 error for each raw and reweighted simulation. The LVBP reduced χ^2 is estimated as the mean reduced χ^2 over all MCMC samples. (b-d). Raw and reweighted conformational propensities for each force field. Note that amber99 shows larger uncertainties due to the extremely limited amount of PP_{II} sampling in the amber99 forcefield.

ands, aggregate, and change conformation. Biology is controlled by the relative populations of these states. Structural ensembles capture aspects of these phenomena by encoding equilibrium populations. A second argument for ensemble modelling is fidelity to experiment. Most solution experiments measure ensemble average equilibrium properties—chemical shifts, scalar couplings, NOEs, SAXS, and FRET are reasonably well-described as equilibrium properties. A truly quantitative connection to these measurements requires modelling the equilibrium ensemble. Finally, recent advances in atomistic simulation,^{17–20} special-purpose hardware,²¹ and distributed computing analysis^{22,23} have enabled atomistic simulations to reach the millisecond timescale;^{24–27} the computational cost of ensemble modeling is quickly becoming manageable.

One might argue that structural ensembles are unnecessary because many proteins occupy a single state under physiological conditions. For such proteins, it is probably safe to enforce single state behavior, as is done in current modelling approaches. However, we suggest that the number of states be *inferred*—not *assumed*.

Comparison to previous methods

LVBP offers several key advantages over previous ensemble estimation techniques. Most previous ensemble modeling efforts involve a protocol that involves three key ingredients: clustering, a χ^2 objective function, and population inference on the clusters. For example, this recipe describes the approach used in previous analyses of homopeptides,² the EROS inference technique,²⁸ and the Bayesian Weighting formalism.⁷ In our opinion, the primary disadvantage of these techniques is the need for a clustering step. The clustering step can introduce two forms of error. First, clustering can overly coarsen the system of interest. For example, too few states could prevent the model from reproducing multiple experimental observables. At the other extreme, too many states could lead to over-fitting and sensitivity to prior—this is because one needs to estimate a large number of populations. This will lead to poor generalization performance—high errors when predicting experiments *not* used to train the model.

In contrast, LVBP avoids clustering by projecting simulations onto a basis defined by the pre-

dicted experimental observables. The advantage of working in this basis are threefold.

First, in LVBP, one estimates a single parameter (α_i) for each experimental observable. If the number of experiments is small, as is often the case, the inference problem has only a few parameters to estimate.

Second, the predicted observables are a *natural* basis for biophysical calculations. This basis allows direct connection to experiment and often provides insight into the molecular interactions driving biophysical phenomena. For example, the projection onto observables could be used to rationally infer forcefield parameters, similar to ForceBalance method.[?]

Third, suppose two conformations have the same predicted experimental observables. In LVBP, these conformations will have the same population. In clustering based methods, the populations of these conformations could vary simply due to random fluctuations.

Finally, in the limit of exact measurements, LVBP gives the same answer as a previous⁶ maximum entropy approach (see Appx. SX).

These reasons provide a theoretical basis supporting the LVBP method. However, it is possible to evaluate the method *quantitatively*. One hallmark of a good statistical model is its predictive ability on set-aside test data.²⁹ We therefore fit BW models on the training data and evaluated on the set-aside test data. For four out of five force fields, we find that the LVBP models outperform the raw MD models and the BW model with few (4) and many (144) states, respectively. Our four state model consists of the (ϕ, ψ) based secondary structure assignments¹⁵ (α_r , β , PP_{II} , and other). Our 144 state model was constructed by dividing the ramachandran plot into square bins of 30×30 degrees. Although the BW models outperform LVBP in one case, this case happens to be for the amber99sbnmr-ildn forcefield. That forcefield was *fit* to match NMR observables; the raw MD simulation has a reduced χ^2 well below 1. This suggests that all methods (raw MD, LVBP, and BW) are consistent with experiment.

	amber96	amber99	amber99sbnmr-ildn	charmm27	oplsaa
maxent	0.776853	0.980453	1.008226	0.931457	1.090944
MVN	0.838097	1.033197	0.942220	0.939043	1.067730
BW	0.973795	1.472812	0.735458	1.061796	1.990149
BW12	1.507146	3.011690	0.469157	1.090342	2.341762
MD	1.508180	3.199790	0.644300	1.161881	2.310684

Conclusion

Bayesian inference of conformational ensembles allows the simultaneous characterization of structural and equilibrium properties. Limited experimental data can be used to supplement equilibrium simulations, leading to predictions that are robust to forcefield error and consistent with available measurements. Our equilibrium ensemble of BPTI suggests coupled motion in the trypsin specificity loop and the C14-C38 disulfide bridge. Falsifying or refining the present model offers a key challenge for understanding the conformational fluctuations in BPTI.

Acknowledgements

We thank John Chodera, TJ Lane, Frank Cochran, Pehr Harbury, Xuesong Shi, and Dan Herschlag for helpful discussions. We thank DE Shaw research for providing the millisecond simulation of BPTI.

Methods

Methods: Trialanine

Trialanine was simulated in the amber96,³⁰ amber99,³¹ amber99sbnmr-ildn,³² charmm27,^{33,34} and oplsaa³⁵ force fields, as previously reported.¹¹ Simulations were performed using Gromacs

4.5¹⁷ and run at constant temperature (300 K) and pressure (1.01 atm). Each simulation was at least 225 ns long. Conformations were stored every 5 ps. Chemical shifts (H, HA, CA, CB) for each frame were calculated using the average prediction of ShiftX2,³⁶ SPARTA+,³⁷ and PPM;³⁸ uncertainties were estimated as the mean uncertainty reported by SPARTA+. J couplings were calculated using the following Karplus relations: $^3J(H^NC')$,³⁹ $^3J(H^NH^\alpha)$,⁴⁰ $^2J(NC^\alpha)$,⁵ $^3J(H^\alpha C')$,³⁹ $^1J(NC^\alpha)$,⁵ $^3J(H^NC^\beta)$ citevogeli2007limits. J coupling uncertainties were approximated as the RMS errors reported when fitting the Karplus coefficients.

References

- (1) Berman, H. M.; Westbrook, J.; Feng, Z.; Gilliland, G.; Bhat, T. N.; Weissig, H.; Shindyalov, I. N.; Bourne, P. E. *Nucleic Acids Res.* **2000**, 28, 235–242.
- (2) Dethoff, E. A.; Petzold, K.; Chugh, J.; Casiano-Negroni, A.; Al-Hashimi, H. M. *Nature* **2012**,
- (3) Fink, A. L. *Current opinion in structural biology* **2005**, 15, 35–41.
- (4) Korzhnev, D. M.; Salvatella, X.; Vendruscolo, M.; Di Nardo, A. A.; Davidson, A. R.; Dobson, C. M.; Kay, L. E. *Nature* **2004**, 430, 586–590.
- (5) Graf, J.; Nguyen, P.; Stock, G.; Schwalbe, H. *J. Am. Chem. Soc.* **2007**, 129, 1179–1189.
- (6) Pitera, J.; Chodera, J. *Journal of Chemical Theory and Computation* **2012**,
- (7) Fisher, C. K.; Huang, A.; Stultz, C. M. *Journal of the American Chemical Society* **2010**, 132, 14919.
- (8) Rieping, W.; Habeck, M.; Nilges, M. *Science* **2005**, 309, 303–306.
- (9) Patil, A.; Huard, D.; Fonnesbeck, C. J. *Journal of statistical software* **2010**, 35, 1.
- (10) Rubin, D. *The annals of statistics* **1981**, 9, 130–134.
- (11) Beauchamp, K.; Lin, Y.; Das, R.; Pande, V. *J. Chem. Theory Comput.* **2012**, 8, 1409.

- (12) Nerenberg, P.; Head-Gordon, T. *J. Chem. Theory Comput.* **2011**, *7*, 1220–1230.
- (13) Best, R.; Buchete, N.; Hummer, G. *Biophys. J.* **2008**, *95*, L07–L09.
- (14) Grdadolnik, J.; Mohacek-Grosov, V.; Baldwin, R.; Avbelj, F. *Proc. Natl. Acad. Sci. U. S. A.* **2011**, *108*, 1794.
- (15) Jha, A.; Colubri, A.; Zaman, M.; Koide, S.; Sosnick, T.; Freed, K. *Biochemistry* **2005**, *44*, 9691–9702.
- (16) Avbelj, F.; Grdadolnik, S.; Grdadolnik, J.; Baldwin, R. *Proc. Natl. Acad. Sci. U. S. A.* **2006**, *103*, 1272.
- (17) Hess, B.; Kutzner, C.; Van Der Spoel, D.; Lindahl, E. *J. Chem. Theory Comput.* **2008**, *4*, 435–447.
- (18) Pronk, S.; Pall, S.; Schulz, R.; Larsson, P.; Bjelkmar, P.; Apostolov, R.; Shirts, M. R.; Smith, J. C.; Kasson, P. M.; van der Spoel, D. *Bioinformatics* **2013**,
- (19) Eastman, P.; Friedrichs, M. S.; Chodera, J. D.; Radmer, R. J.; Bruns, C. M.; Ku, J. P.; Beauchamp, K. A.; Lane, T. J.; Wang, L.-P.; Shukla, D.; Pande, V. S. *Journal of chemical theory and computation* **2012**, *9*, 461–469.
- (20) Eastman, P.; Pande, V. *Comp. in Sci. Eng.* **2010**, *12*, 34–39.
- (21) Shaw, D.; Deneroff, M.; Dror, R.; Kuskin, J.; Larson, R.; Salmon, J.; Young, C.; Batson, B.; Bowers, K.; Chao, J. *Commun. ACM* **2008**, *51*, 91–97.
- (22) Senne, M.; Trendelkamp-Schroer, B.; Mey, A. S. J. S.; Schütte, C.; Noé, F. *J. Chem. Theory Comput.* **2012**,
- (23) Beauchamp, K.; Bowman, G.; Lane, T.; Maibaum, L.; Haque, I.; Pande, V. *J. Chem. Theory Comput.* **2011**, *7*, 3412–3419.
- (24) Voelz, V.; Bowman, G.; Beauchamp, K.; Pande, V. *J. Am. Chem. Soc.* **2010**, *132*, 1526–1528.

- (25) Bowman, G. R.; Voelz, V. A.; Pande, V. S. *Journal of the American Chemical Society* **2011**, *133*, 664.
- (26) Shaw, D. E.; Maragakis, P.; Lindorff-Larsen, K.; Piana, S.; Dror, R. O.; Eastwood, M. P.; Bank, J. A.; Jumper, J. M.; Salmon, J. K.; Shan, Y.; Wriggers, W. *Science* **2010**, *330*, 341–346.
- (27) Lindorff-Larsen, K.; Piana, S.; Dror, R.; Shaw, D. *Science* **2011**, *334*, 517–520.
- (28) Rozycki, B.; Kim, Y. C.; Hummer, G. *Structure* **2011**, *19*, 109–116.
- (29) Friedman, J.; Hastie, T.; Tibshirani, R. *The elements of statistical learning*; Springer Series in Statistics, 2001; Vol. 1.
- (30) Kollman, P. *Acc. Chem. Res.* **1996**, *29*, 461–469.
- (31) Wang, J.; Cieplak, P.; Kollman, P. *J. Comput. Chem.* **2000**, *21*, 1049–1074.
- (32) Li, D.; Bruschweiler, R. *Angew. Chem.* **2010**, *122*, 6930–6932.
- (33) Mackerell Jr, A.; Feig, M.; Brooks III, C. *J. Comput. Chem.* **2004**, *25*, 1400–1415.
- (34) Bjelkmar, P.; Larsson, P.; Cuendet, M.; Hess, B.; Lindahl, E. *J. Chem. Theory Comput.* **2010**, *6*, 459–466.
- (35) Kaminski, G.; Friesner, R.; Tirado-Rives, J.; Jorgensen, W. *J. Phys. Chem. B* **2001**, *105*, 6474–6487.
- (36) Han, B.; Liu, Y.; Ginzinger, S.; Wishart, D. *J. Biomol. NMR* **2011**, 1–15.
- (37) Shen, Y.; Bax, A. *J. Biomol. NMR* **2010**, *48*, 13–22.
- (38) Li, D.-W.; Bruschweiler, R. *Journal of Biomolecular NMR* **2012**, 1–9.
- (39) Schmidt, J.; Blümel, M.; Löhr, F.; Rüterjans, H. *J. Biomol. NMR* **1999**, *14*, 1–12.

- (40) Vögeli, B.; Ying, J.; Grishaev, A.; Bax, A. *Journal of the American Chemical Society* **2007**, *129*, 9377–9385.